crystals

MDPI

Article

# Synthesis, Crystal Structure, and Solubility Analysis of a Famotidine Cocrystal

**Yan Zhang [1,2,*], Zhao Yang [2], Shuaihua Zhang [3] and Xingtong Zhou [2]**

1 School of Medicine and Pharmacy, Ocean University of China, Qingdao 266003, China
2 Qingdao Institute for Food and Drug Control, Qingdao 266071, China
3 School of Pharmacy, Qingdao University, Qingdao 266071, China
* Correspondence: yanzhang139@139.com; Tel.: +86-532-5875-9178

Received: 15 May 2019; Accepted: 10 July 2019; Published: 15 July 2019


**Abstract:** A novel cocrystal of the potent $H_2$ receptor antagonist famotidine (FMT) was synthesized with malonic acid (MAL) to enhance its solubility. The cocrystal structure was characterized by X-ray single crystal diffraction, and the asymmetry unit contains one FMT and one MAL connected via intermolecular hydrogen bonds. The crystal structure is monoclinic with a P21/n space group and unit cell parameters a = 7.0748 (3) Å, b = 26.6502 (9) Å, c = 9.9823 (4) Å, $\alpha$ = 90, $\beta$ = 104.2228 (12), $\gamma$ = 90, V = 1824.42 (12) Å$^3$, and Z = 4. The cocrystal had unique thermal, spectroscopic, and powder X-ray diffraction (PXRD) properties that differed from FMT. The solubility of the famotidine-malonic acid cocrystal (FMT-MAL) was 4.2-fold higher than FMT; the FAM-MAL had no change in FMT stability at high temperature, high humidity, or with illumination.

**Keywords:** cocrystal; famotidine; malonic acid; crystal structure; solubility

## 1. Introduction

Drugs with low water solubility usually show dissolution-limited absorption and low bioavailability [1]. Recent estimates suggest that approximately 40% of currently marketed drugs and up to 75% of compounds currently under development are poorly water soluble; thus, enhancing the aqueous solubility of poorly water-soluble active pharmaceutical ingredients (APIs) is a key challenge for pharmaceutical scientists [2]. Salts are historically the first choice for overcoming poor solubility and dissolution rate problems in APIs. However, cocrystals have recently emerged as a subject of intense research [3].

In the past decade, cocrystal technology emerged as an advanced approach to enhance the aqueous solubility of poorly water-soluble drugs via crystal engineering principles without changing their chemical structure [4–12]. A pharmaceutical cocrystal is defined as a multicomponent molecular complex combining an API and coformer(s) through non-covalent interactions (e.g., hydrogen bonding, van der Waals forces, $\pi$-stacking, and electrostatic interactions) in a definite stoichiometric ratio [13,14]. Distinctions between salts and cocrystals can be made based on whether a proton transfer has occurred from an acid to a base [15]. However, the determination of whether a salt or a cocrystal has formed can be difficult. Crystal structure determination often does not afford accurate proton positions, and other techniques are, therefore, often necessary [16].

Famotidine(3-[({2-[(Hydrazonomethyl)amino]thiazol-4-yl}methyl)thio]-*N*-sulfamoylpropionamidine) (FMT, pKa = 7.06) (Figure 1) is a potent $H_2$ receptor antagonist commonly used for gastroesophageal reflux disease [17]. It is insoluble in cold water, and this poor aqueous solubility may contribute to its low and variable oral bioavailability [18]. FMT exhibits two major crystalline polymorphs (forms A and B), where B is the metastable form [19]. Several studies have suggested that cocrystal solubility can correlate strongly with coformer solubility [20], thus, we describe here a water-soluble organic acid—Malonic acid

(MAL; $pKa_1$ = 2.8, $pKa_2$ = 5.7) (Figure 1). This was selected as cocrystal coformer (CCF) to synthesize a novel cocrystal with FMT. Single crystal X-ray diffraction, Fourier transform infrared spectroscopy (FT-IR), and conductivity experiments were performed to identify that it is a cocrystal instead of a salt. Furthermore, the cocrystal of FMT with MAL (FMT-MAL) showed a 4.2-fold increase in FMT solubility without changing its stability.

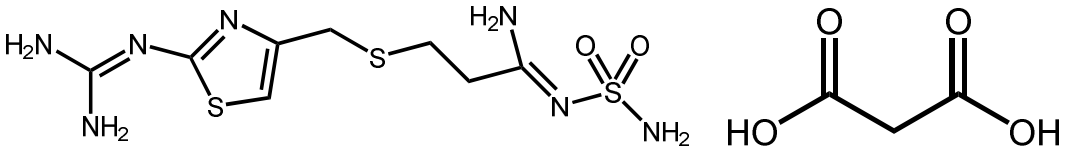


(**a**) (**b**)

**Figure 1.** Structures of (**a**) FMT and (**b**) MAL.

## 2. Experimental Section

### *2.1. General*

FMT (drug substance, form B) was supplied by Qingdao Liteng Chemical Medical Research Co., Ltd (Qingdao, China). A reference standard of FMT (100305–201304, 99.5% purity) was purchased from National Institutes for Food and Drug Control. High-pressure liquid chromatography (HPLC) grade methanol and acetonitrile were purchased from Merck (Darmstadt, Germany). MAL and the other chemicals were purchased from Sinopharm Chemical Reagent Co., Ltd. (Shanghai, China). Powder diffractograms were recorded on a Bruker D8 Focus with a Cu-K$\alpha$ radiation (1.54060 Å). A simulated powder X-ray diffraction (PXRD) pattern was calculated from the refined single crystal structures of FMT-MAL by Mercury 4.0.0. A Spectrum65 FT-IR spectrometer (Perkin Elmer) was employed in the KBr diffuse-reflectance mode (sample concentration was 2 mg in 20 mg of KBr) for collecting the IR spectra of the sample. Differential scanning calorimetry (DSC) used a DSC6000 (Perkin Elmer, Waltham, Massachusetts, USA)). Thermogravimetric analysis (TGA) was performed using a TGA8000 instrument (Perkin Elmer, Waltham, MA, USA).

### *2.2. Synthesis of FMT-MAL Cocrystal*

FMT (340 mg, 1 mmol) was dissolved in a mixture of methanol (7 mL) and dimethylformamide (3 mL) and heated and stirred at 70 °C for 1 h. MAL (104 mg, 1 mmol) was added and stirred at 70 °C for 2 h. The resulting solution was filtered and allowed to slowly evaporate at room temperature for 2 days. Single crystals were carefully selected under a microscope and kept in mineral oil.

### *2.3. Single-Crystal X-ray Diffraction Analysis*

X-ray reflections were collected on a D8 Quest diffractometer (Bruker, Rheinstetten, Germany) equipped with a PHOTON II CPAD detector using Co radiation (0.71073 Å) at room temperature (296 K). Data were corrected via a $\omega$ scan, and the absorption effects were studied using the multi-scan method. The structure was solved with the ShelXT [21] structure solution program using direct methods and refined with the XL [22] refinement package using Least Squares minimization. Anisotropical thermal factors were assigned to all of the non-hydrogen atoms. The positions of the hydrogen atoms were generated geometrically.

### *2.4. Conductivity*

Conductivity was measured using a Sioinlab740 conductivity meter (Mettler Toledo, Greifensee, Switzerland). FMT-MAL (52 mg) and a mixture of FMT (40 mg) and MAL (12 mg) were both dissolved in 35 mL water.

### 2.5. High-Pressure Liquid Chromatography (HPLC)

A solution of each sample (for solubility and stability experiments) was analyzed via a1260 HPLC system (Agilent Technologies, Santa Clara, California, USA) equipped with a diode array detector (set at 270 nm). The chromatographic separation used an Agilent ZORBAX SB-C18 5 µm column (4.6 mm × 250 mm) at 35 °C. The mobile phase consisted of sodium acetate buffer (13.6 mg $mL^{-1}$, pH = 6.0 ± 0.1) and acetonitrile (93:7 in volume) at a flow rate of 1.5 mL $min^{-1}$.

### 2.6. Solubility Determination

The solid samples for solubility studies were sieved (150 µm ± 6.6 µm diameter mesh sieve) to obtain uniform particle size. The solubility was determined by suspending 500 mg of the solid samples in 100 mL of water at 25 °C and 100 rpm in 708-DS dissolution apparatus (Agilent Technologies, Santa Clara, CA, USA) with a paddle method. Samples (1 mL) were collected at 5, 10, 20, 30, 45, 60, 90,120, 240, 360, 480, 600, 720, 840, 960, 1080, 1200, 1320, and 1440 min, and then filtered through a 0.45-µm nylon filter and assayed for drug content by HPLC.

### 2.7. Stability Determination

We next tested the stability at high relative moisture content, high temperature, and high illumination conditions. The FMT and FMT-MAL were stored in a SHH-SDF stability chamber (Yongsheng, Chongqing, China) at 60 °C, 25 °C/92.5% relative humidity (RH), and 4500 lux conditions for 10 days. Samples were collected at 0, 5, and 10 days, and analyzed by HPLC to assay for chemical purity.

## 3. Results and Discussion

### 3.1. Crystal Strcture

The cocrystal showed unique peaks in PXRD that differed from its raw components, indicating that a new cocrystal was formed. The PXRD pattern of FMT-MAL showed new peaks at 2θ values of 14.2°, 16.2°, 18.5°, 21.6°, 22.0°, 27.8°, and 29.8°, which were not present in FMT and MAL (Figure 2). A further comparison between the simulated PXRD pattern and the experimental PXRD pattern of FMT-MAL showed a definitive match indicating the homogeneity and purity of FMT-MAL crystalline phase.

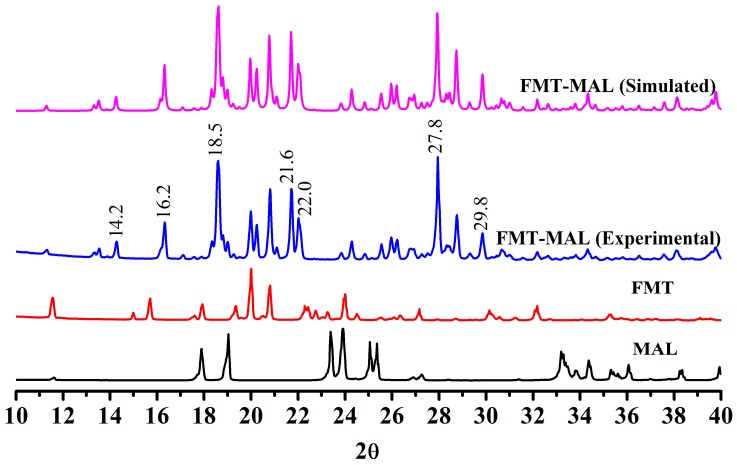


**Figure 2.** PXRD patterns of FMT-MAL (simulated), FMT-MAL (experimental), FMT, and MAL.

The FMT-MAL was a colorless block, unlike the colorless needle of FMT. X-ray structural analyses revealed that FMT-MAL crystallizes in a non-standard space group ($P2_1/n$). Crystal data for FMT-MAL are summarized in Table 1. Selected bond lengths and angles for FMT-MAL are listed in Table 2. The asymmetric units of FMT-MAL consist of one molecule of FMT and one molecule of MAL (Figure 3a).

There are three kinds of intermolecular H-bonds within the molecular units (Figure 3b). The first and second ones share the same donor atom (N1). The first one is N1–H1A···O2 (pick dotted line, $d_{N\cdots O}$ = 2.827 (1) Å; ∠NHO = 145°). The second one is N1–H2B···O3 (green dotted line, $d_{N\cdots O}$ = 2.796 (1) Å; ∠NHO = 171.00°). Here, the O3 from the carbonyl group of MAL is the acted as an acceptor. The third H-bond originates from N2–H2A···O6 (turquoise dotted line, $d_{N\cdots O}$ = 2.837 (1) Å; ∠NHO = 167°), in which the O6 from the carbonyl group of MAL acted as an acceptor. The fourth hydrogen bond originates from N5–H5B···O1 (black dotted line, $d_{N\cdots O}$ = 2.860 (1) Å; ∠NHO = 157°). Here, the O1 from sulfanilamide group acted as an acceptor. The hydrogen bonds for FMT-MAL are listed in Table 3. The hydrogen bonding interactions in the structure of FMT-MAL allowed the FMT and MAL to connect in a molecular way and expand the networks to three dimensions (Figure 3c). The crystallographic data, in CIF format, was deposited with the Cambridge Crystallographic Data Centre, CCDC 1576773.

**Table 1.** Crystal data and structure refinements.

| Compound | FMT-MAL |
|---|---|
| Formula | $C_{11}H_{19}N_7O_6S_3$ |
| Formula Weight | 441.51 |
| Temperature (K) | 296 (2) |
| Crystal System | Monoclinic |
| Space Group | $P2_1/n$ |
| a (Å) | 7.0748 (3) |
| b (Å) | 26.6502 (9) |
| c (Å) | 9.9823 (4) |
| α ° | 90 |
| β ° | 104.2228 (12) |
| γ ° | 90 |
| Volume (Å$^3$) | 1824.42 (12) |
| Z | 4 |
| Density calculated (g·cm$^{-3}$) | 1.607 |
| F (000) | 920 |
| Absorption coefficient (mm$^{-1}$) | 0.453 |
| Reflection collected | 25641 |
| Unique Reflection | 8367 |
| $R_{int}$ | 4189 |
| $R_1$ [a], $wR_2$ [b] [I > 2σ(I)] | 0.0544/0.1477 |
| $R_1$, $wR_2$ (all data) | 0.0691/0.1586 |
| Goodness-of-fit on F$^2$ | 1.049 |
| $\Delta\rho_{max}$, $\Delta\rho_{min}$, (e Å$^{-3}$) | 0.617, −0.559 |

Note: [a] $R_1=\Sigma||F_o|-|F_c||/\Sigma|F_o|$, [b] $wR_2=[\Sigma w(F_o^2-F_c^2)^2/\Sigma w(F_o^2)^2]^{1/2}$.

**Table 2.** Selected Bond Lengths (Å), Angles (°), and Torsion angles (°).

| FMT-MAL | | | |
|---|---|---|---|
| S (1)-C (3) | 1.719 (3) | S (1)-C (2) | 1.723 (2) |
| S (2)-C (6) | 1.805 (3) | S (2)-C (5) | 1.814 (3) |
| S (3)-O (1) | 1.432 (2) | S (3)-N (6) | 1.613 (2) |
| S (3)-O (2) | 1.438 (2) | S (3)-N (7) | 1.609 (3) |
| C (9)-O (3) | 1.222 (4) | C (11)-O (5) | 1.300 (4) |
| C (9)-O (4) | 1.278 (4) | C (11)-O (6) | 1.215 (4) |
| N (3)-C (1) | 1.355 (3) | N (3)-C (2) | 1.391 (3) |
| N (4)-C (2) | 1.295 (3) | N (4)-C (4) | 1.391 (3) |
| O (1)-S (3)-N (7) | 109.30 (15) | C (1)-N (3)-C (2) | 125.2 (2) |
| O (2)-S (3)-N (7) | 105.97 (13) | C (18)-N (2)-C (21) | 108.02 (14) |
| O (1)-S (3)-N (6) | 105.50 (12) | N (2)-C (1)-N (1) | 122.0 (2) |
| O (2)-S (3)-N (6) | 113.49 (12) | N (2)-C (1)-N (3) | 121.0 (2) |
| N (7)-S (3)-N (6) | 106.09 (13) | N (1)-C (1)-N (3) | 117.0 (2) |
| O (1)-S (3)-N (6)-C (8) | | −168.8 (2) | |
| O (2)-S (3)-N (6)-C (8) | | −40.7 (3) | |
| N (7)-S (3)-N (6)-C (8) | | 75.2 (2) | |

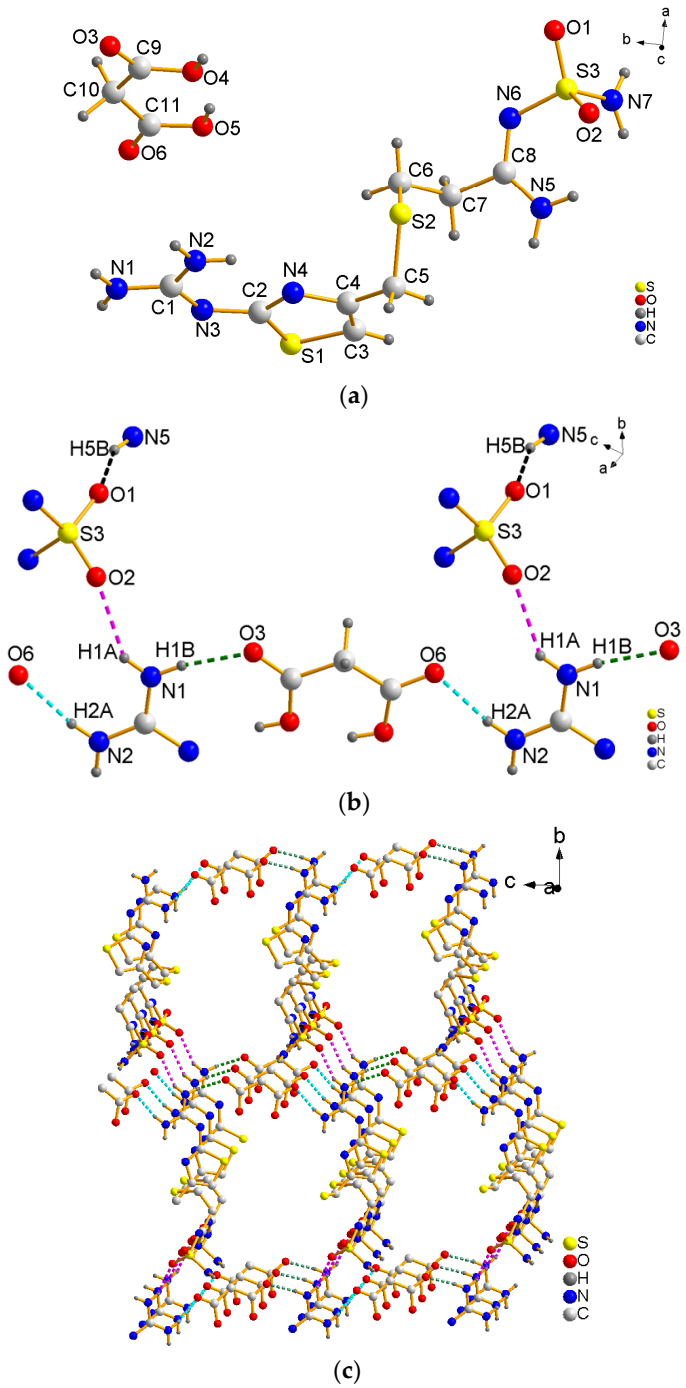


**Figure 3.** (**a**) View of the asymmetric unit of FMT-MAL, (**b**) hydrogen bonds in FMT-MAL, and (**c**) view of the 3D supramolecular structure of FMT-MAL.

**Table 3.** Hydrogen-bond geometries and interactions for FMT-MAL.

| Hydrogen Bond | Distance [a], Å | Distance [b], Å | Angle [c], ° |
|---|---|---|---|
| N1–H1A···O2 | 2.18 | 2.927 (1) | 145 |
| N1–H1B···O3 | 1.94 | 2.796 (1) | 171 |
| N2–H2A···O6 | 1.99 | 2.837 (1) | 167 |
| N5–H5B···O1 | 2.05 | 2.860 (1) | 157 |

Note: [a] Distance between donor and acceptor; [b] distance between hydrogen and acceptor; [c] angle of acceptor–hydrogen–donor.

During the structure analysis, N3 of guanidine was found to show approximately 0.65e/Å$^3$ residual electron, which is located approximately 0.93 Å positions from N3 toward O4 of malonic acid. The distance of C1–N3 is 1.355 (3) Å. This is much shorter than the distance of C–N in [C = NH$^+$] (1.371 (1) Å) versus the reported structure of FMT-HCl [23]. This suggests that the N3 atom from C = N group has not been protonated. The carbonyl groups of malonic acid have shorter bond lengths (C9-O3 = 1.222 (4) Å and C11-O6 = 1.215 (4) Å) and C–OH groups of malonic acid have larger bond lengths (C9-O4 = 1.278 (4) Å and C11-O5 = 1.300 (4) Å). Thus, malonic acid in the cocrystal exists as a neutral moiety (no proton was transfer occurred), which is evident from the carboxylic acid bond length [24–26]. Therefore, the residual electron around N3 was rejected as a hydrogen atom, and one hydrogen atom was calculated on O4 to make the malonic acid a neutral molecule and not the anion form. The flat conformation of the neutral malonic acid molecule, which has two OH groups (O4 and O5) on the same side of the molecule, is reported in a few structures, such as CUVDON, CUVDON01, EPERIP, UFETOR, UFEVUZ, and URMALN (ConQuest Version 2.0.0), thus it is not rare. Further study of the sulfanilamide group showed that the distances of S3–N6 and S3–N7 are 1.613 (2) Å and 1.609 (3) Å, respectively. The N7–S3–N6 bridging angle is 106.09 (13)°. The distances and angles are comparable to reported FMT crystal structure, suggesting that the $NH_2$ from the sulfanilamide group has not been protonated [27]. In addition, we performed conductivity experiments. The conductivity studies showed that the solution of FMT-MAL had a lower conductivity (190.3 μS cm$^{-1}$) than the mixture of FMT and MAL at a molar ratio of 1:1 (244.7 μS cm$^{-1}$). The lower conductivity suggests that FMT-MAL may still be connected together via weak interactions in the water. Thus, the results of the conductivity experiment suggest that FMT-MAL is a cocrystal rather than a salt at room temperature.

### *3.2. Thermal Properties*

DSC analysis revealed that FMT-MAL had a unique melting point at 172.5 °C, which was higher than the melting points of both FMT (163.6 °C) and MAL (135.3 °C) (Figure 4a). It is common that the cocrystal shows an intermediate melting point between the API and conformer. However, a study showed that within the survey, 50 cocrystalline samples were analyzed, and 3 out of 50 (6%) had melting points higher than either the API or conformer. Higher thermal stability of the cocrystal could be associated to crystal packing [28]. The TGA curves show that FMT-MAL had an onset decomposition temperature of 180.0 °C. There was no significant change in the weight before an endothermic phenomenon occurred. This confirmed its non-solvated character and high purity (Figure 4b).

### *3.3. Fourier Transform Infrared Spectroscopy*

Infrared spectroscopy is a powerful tool for detecting cocrystal formation because the vibrational changes serve as probes for intermolecular interactions in solid materials [28]. The famotidine showed peaks at 3505, 3399, and 3376 cm$^{-1}$, corresponding to the –NH stretch. There are decreases in the –N–H stretching frequency of famotidine at 3389, 3342, and 3246 cm$^{-1}$ in the cocrystal. The peak of malonic acid at 1700 cm$^{-1}$ corresponds to the –C=O stretch and moved to high-frequency (1721 cm$^{-1}$) in the cocrystal (Figure 5). This suggests that the –N–H group of famotidine and the –C=O group of malonic acid participants have some interactions. The results were coincident with the single-crystal X-ray diffraction data. Furthermore, a rapid means of establishing the formation of a salt or a cocrystal of FMT with MAL is by detection of shifts in ν (C = O) for the MAL. An indication of cocrystal formation is the occurrence of a shift of C = O group of malonic acid to higher energies (from1700 cm$^{-1}$ to 1721 cm$^{-1}$) [3].

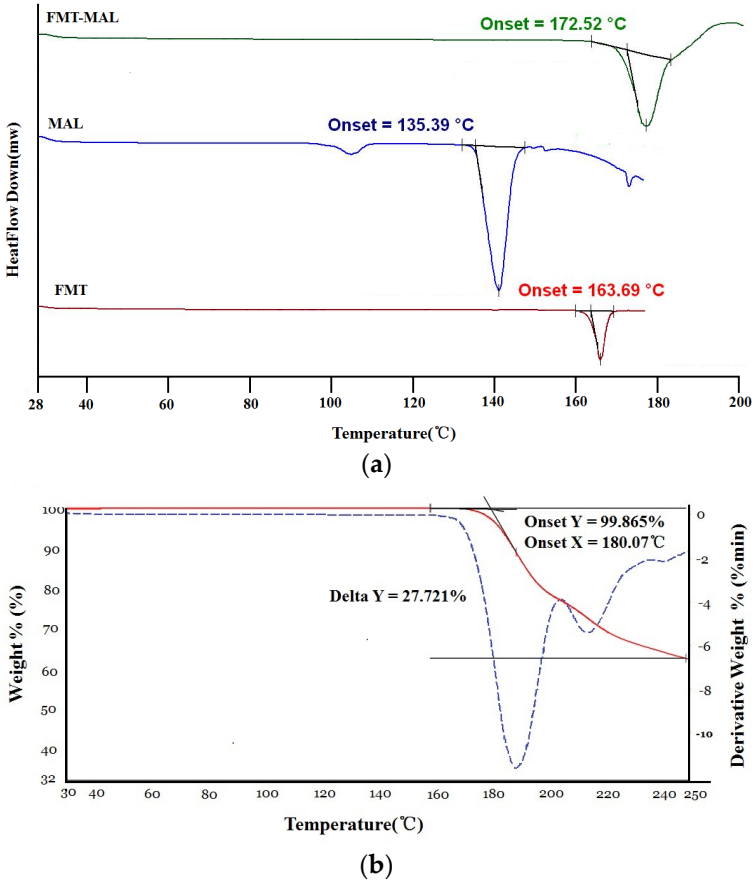


**Figure 4.** (**a**) DSC and (**b**) TGA thermograms of FMT-MAL.

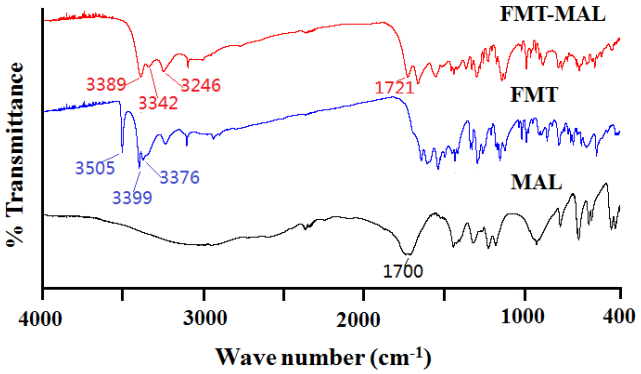


**Figure 5.** IR spectra of the FMT-MAL, FMT, and MAL.

### *3.4. Aqueous Solubility*

The maximum famotidine concentration was determined to be 0.96 mg $mL^{-1}$ after 8 h. The solubility enhancement was demonstrated via the FMT-MAL cocrystal—the maximum concentration of FMT was 4.06 mg $mL^{-1}$ after 30 min. Thus, the FMT-MAL showed a 4.2-fold increase versus parent FMT (Figure 6). The cocrystal was stable for more than 24 h, as confirmed by analyzing undissolved material using PXRD (Figure 7).

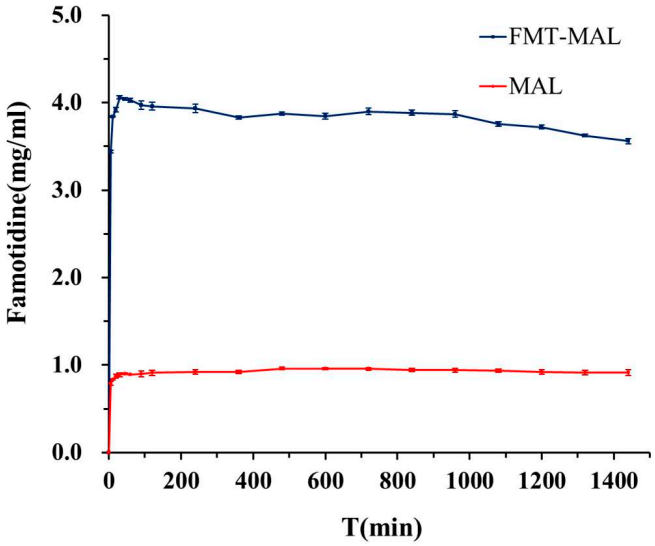


**Figure 6.** Solubility curves of FMT and FMT-MAL.

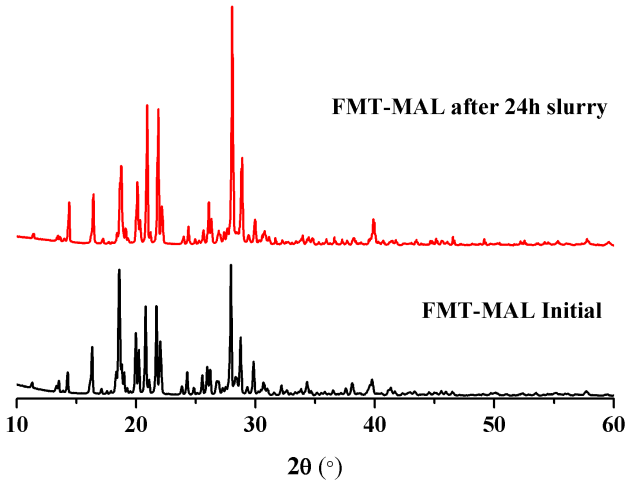


**Figure 7.** PXRD patterns of FMT-MAL and product after 24 h in a slurry of water.

### *3.5. Stability*

The stability studies of FMT and FMT-MAL at 60 °C, 25 °C/92.5% RH, and 4500 lux conditions indicated that the cocrystal did not change the stability of FMT (Table 4).

**Table 4.** Stability data at 60 °C, 25 °C/92.5% RH, and 4500 lux conditions.

| FMT | Inspection Item | 0 Day | 5 Day | 10 Day |
|---|---|---|---|---|
| 4500 lux | Content (%) | 99.8 | 99.4 | 98.9 |
| 60 °C | Content (%) | 99.8 | 99.2 | 98.2 |
| 25 °C, 92.5% RH | Increasing Weight (%) | 0 | 0.005 | 0.008 |
| | Content (%) | 99.8 | 98.8 | 97.6 |
| **FMT-MAL** | **Inspection Item** | **0 Day** | **5 Day** | **10 Day** |
| 4500 lux | Content (%) | 99.5 | 99.3 | 99.0 |
| 60 °C | Content (%) | 99.5 | 98.2 | 97.5 |
| 25 °C, 92.5% RH | Increasing Weight (%) | 0 | 0.007 | 0.010 |
| | Content (%) | 99.5 | 98.6 | 98.5 |

## 4. Conclusions

In summary, we describe a novel cocrystal of FMT obtained by co-crystallization with MAL. This improves its solubility. The cocrystal was characterized by single-crystal X-ray diffraction. The crystal structure was monoclinic with a P21/n space group; the asymmetry unit contained a FMT and a MAL connected via intermolecular hydrogen bonds between the amide of famotidine and the carboxy of malonic acid. The FMT-MAL had unique thermal, spectroscopic, and PXRD properties that differed from FMT. The FMT-MAL improved the aqueous solubility of famotidine. There was a 4.2-fold increase in FMT solubility with no impact on stability. This new cocrystal can improve the bioavailability of FMT but additional trials are needed to confirm it. These results offer further insight into the co-crystallization in terms of both supramolecular chemistry and solubility modification.

**Author Contributions:** Data curation, Y.Z., Z.Y., and X.Z.; methodology, Y.Z. and S.Z.; writing—original draft, Y.Z.; writing—review and editing, Y.Z. and Z.Y.

**Funding:** This research received no external funding.

**Conflicts of Interest:** The authors declare no conflict of interest.

## References

1. Kawabata, Y.; Wada, K.; Nakatani, M.; Yamadaa, S.; Onouea, S. Formulation design for poorly water-soluble drugs based on biopharmaceutics classification system: Basic approaches and practical applications. *Int. J. Pharm.* **2011**, *420*, 1–10. [CrossRef] [PubMed]
2. Williams, H.D.; Trevaskis, N.L.; Charman, S.A.; Shanker, R.M.; Charman, W.N.; Pouton, C.W.; Porter, C.J.H. Strategies to address low drug solubility in discovery and development. *Pharmacol. Rev.* **2013**, *65*, 315–499. [CrossRef] [PubMed]
3. Mittapalli, S.; Mannava, M.K.C.; Khandavilli, U.B.R.; Allu, S.; Nangia, A. Soluble salts and cocrystals of clotrimazole. *Cryst. Growth Des.* **2015**, *15*, 2493–2504. [CrossRef]
4. Park, B.; Yoon, W.; Yun, J.; Ban, E.; Yun, H.; Kim, A. Emodin-nicotinamide (1:2) cocrystal identified by thermal screening to improve emodin solubility. *Int. J. Pharm.* **2019**, *557*, 26–35. [CrossRef] [PubMed]
5. Gao, Y.; Zu, H.; Zhang, J. Enhanced dissolution and stability of adefovir dipivoxil by cocrystal formation. *J. Pharm. Pharmacol.* **2011**, *63*, 483–490. [CrossRef] [PubMed]
6. Mcnamara, D.P.; Childs, S.L.; Giordano, J.; Iarriccio, A.; Cassidy, J.; Shet, M.S.; Mannion, R.; O'Donnell, E.; Park, A. Use of a glutaric acid cocrystal to improve oral bioavailability of a low solubility API. *Pharm. Res.* **2006**, *23*, 1888–1897. [CrossRef] [PubMed]
7. Zeng, Q.Z.; Ouyang, J.; Zhang, S.; Zhang, L. Structural characterization and dissolution profile of mycophenolic acid cocrystals. *Eur. J. Pharm. Sci.* **2017**, *102*, 140–146. [CrossRef] [PubMed]
8. Stavropoulos, K.; Johnston, S.C.; Zhang, Y.G.; Rao, B.G.; Hurrey, M.; Hurter, P.; Topp, E.M.; Kadiyala, I. Cocrystalline solids of telaprevir with enhanced oral absorption. *J. Pharm. Sci.* **2015**, *104*, 3343–3350. [CrossRef]
9. Wyche, T.P.; Alvarenga, R.F.R.; Piotrowski, J.S.; Duster, M.N.; Warrack, S.R.; Cornilescu, G.; De Wolfe, T.J.; Hou, Y.; Braun, D.R.; Ellis, G.A.; et al. Chemical genomics, structure elucidation, and in vivo studies of the marine-derived anticlostridial ecteinamycin. *ACS Chem. Biol.* **2017**, *12*, 2287–2295. [CrossRef]
10. Sowa, M.; Slepokura, K.; Matczakjon, E.; Sowa, M.; Ślepokura, K.; Matczak-Jon, E.J.C. Improving solubility of fisetin by cocrystallization. *Cryst. Eng. Comm.* **2014**, *16*, 10592–10601. [CrossRef]
11. Drozd, K.V.; Manin, A.N.; Churakov, A.V.; Perlovich, G.L. Drug-drug cocrystals of antituberculous 4-aminosalicylic acid: Screening, crystal structures, thermochemical and solubility studies. *Eur. J. Pharm. Sci.* **2017**, *99*, 228–239. [CrossRef] [PubMed]
12. Chadha, R.; Bhandari, S.; Haneef, J.; Khullar, S.; Mandal, S. Cocrystals of telmisartan: Characterization, structure elucidation, in vivo and toxicity studies. *Cryst. Eng. Comm.* **2014**, *16*, 8375–8389. [CrossRef]
13. Qiao, N.; Li, M.; Schlindwein, W.; Malek, N.; Davies, A.; Trappitt, G. Pharmaceutical cocrystals: An overview. *Int. J. Pharm.* **2011**, *419*, 1–11. [CrossRef] [PubMed]
14. Miroshnyk, I.; Mirza, S.; Sandler, N. Pharmaceutical co-crystals-an opportunity for drug product enhancement. *Expert Opin. Drug Del.* **2009**, *6*, 333–341. [CrossRef] [PubMed]

15. Childs, S.L.; Stahly, G.P.; Park, A. The salt-cocrystal continuum: The influence of crystal structure on ionization state. *Mol. Pharm.* **2007**, *4*, 323–338. [CrossRef] [PubMed]
16. Cerreia Vioglio, P.; Chierotti, M.R.; Gobetto, R. Pharmaceutical aspects of salt and cocrystal forms of APIs and characterization challenges. *Adv. Drug Deliv. Rev.* **2017**, *117*, 86–110. [CrossRef] [PubMed]
17. Rad, T.S.; Khataee, A.; Kayan, B.; Kalderis, D.; Akay, S. Synthesis of pumice-$TiO_2$ nanoflakes for sonocatalytic degradation of famotidine. *J. Clean Prod.* **2018**, *202*, 853–862. [CrossRef]
18. Mady, F.M.; Abou-Taleb, A.E.; Khaled, K.A.; Yamasaki, K.; Iohara, D.; Ishiguro, T.; Hirayama, F.; Kaneto, U.; Otagiri, M. Enhancement of the aqueous solubility and masking the bitter taste of famotidine using drug/SBE-β-CyD/povidone K30 complexation approach. *J. Pharm. Sci.* **2010**, *99*, 4285–4294. [CrossRef]
19. Német, Z.; Hegedűs, B.; Szántay, C.; Sztatisz, J.; Pokol, G. Pressurization effects on the polymorphic forms of famotidine. *Thermochim. Acta* **2005**, *430*, 35–41. [CrossRef]
20. Karashima, M.; Kimoto, K.; Yamamoto, K.; Kojima, T.; Ikeda, Y. A novel solubilization technique for poorly soluble drugs through the integration of nanocrystal and cocrystal technologies. *Eur. J. Pharm. Biopharm.* **2016**, *107*, 142–150. [CrossRef]
21. Sheldrick, G.M. SHELXT–Integrated space-group and crystal-structure determination. *Acta Crystallogr. A Found. Adv.* **2015**, *71*, 3–8. [CrossRef] [PubMed]
22. Sheldrick, G.M. Crystal structure refinement with SHELXL. *Acta Crystallogr. C Struct. Chem.* **2015**, *71*, 3–8. [CrossRef] [PubMed]
23. Ishida, T.; In, Y.; Doi, M.; Inoue, M.; Yanagisawa, I. Structural study of histamine H2-receptor antagonists. Five 3-[2-(diaminomethyleneamino)-4-thiazolylmethylthio] propionamidine and-amide derivatives. *Acta Crystallogr. B Struct. Sci.* **1989**, *45*, 505–512. [CrossRef] [PubMed]
24. Lemmerer, A.; Bernstein, J.; Kahlenberg, V. One-pot covalent and supramolecular synthesis of pharmaceutical co-crystals using the API isoniazid: A potential supramolecular reagent. *CrystEngComm* **2010**, *12*, 2856–2864. [CrossRef]
25. Noonan, T.J.; Chibale, K.; Cheuka, P.M.; Bourne, S.A.; Caira, M.R. Cocrystal and salt forms of an imidazopyridazine antimalarial drug lead. *J. Pharm. Sci.* **2019**, *108*, 2349–2357. [CrossRef]
26. Shimpi, M.R.; Alhayali, A.; Cavanagh, K.L.; Rodríguez-Hornedo, N.; Velaga, S.P. Tadalafil–malonic acid cocrystal: Physicochemical characterization pH-solubility, and supersaturation studies. *Cryst. Growth Des.* **2018**, *18*, 4378–4387. [CrossRef]
27. Yanagisawa, I.; Hirata, Y.; Ishii, Y. Studies on histamine $H_2$ receptor antagonists. 2. Synthesis and pharmacological activities of N-sulfamoyl and N-sulfonyl amidine derivatives. *J. Med. Chem.* **1987**, *30*, 1787–1793. [CrossRef]
28. Schultheiss, N.; Newman, A. Pharmaceutical cocrystals and their physicochemical properties. *Cryst. Growth Des.* **2009**, *9*, 2950–2967. [CrossRef]